

A Combined Experimental and Theoretical Study of Uranium Polyhydrides with New Evidence for the Large Complex $\text{UH}_4(\text{H}_2)_6$

Juraj Raab,[†] Roland H. Lindh,[‡] Xuefeng Wang,[§] Lester Andrews,[§] and Laura Gagliardi^{*,†}

Department of Physical Chemistry, University of Geneva, 30 Quai Ernest Ansermet, CH-1211 Geneva, Switzerland, Department of Theoretical Chemistry Chemical Center, Lund University, P.O.B. 124, S-22100 Lund, Sweden, and Department of Chemistry, University of Virginia, P.O. Box 400319, 22904-4319 Charlottesville, Virginia

Received: February 15, 2007; In Final Form: April 18, 2007

Several monouranium and diuranium polyhydride molecules were investigated using quantum chemical methods. The infrared spectra of uranium and hydrogen reaction products in condensed neon and pure hydrogen were measured and compared with previous argon matrix frequencies. The calculated molecular structures and vibrational frequencies were used to identify the species present in the matrix. Major new absorptions were observed and compared with the previous argon matrix study. Spectroscopic evidence was obtained for the novel complex, $\text{UH}_4(\text{H}_2)_6$, which has potential interest as a metal hydride with a large number of hydrogen atoms bound to uranium. Our calculations show that the series of complexes $\text{UH}_4(\text{H}_2)_{1,2,4,6}$ are stable.

Introduction

The multiple bond between two U atoms in the U_2 diatomic molecule, and in other earlier diactinides, Ac_2 , Th_2 , and Pa_2 , has been recently investigated by *ab initio* quantum chemistry.¹ The U_2 dication, U_2^{2+} , has also been studied,² together with some possible molecules including the U_2 moiety, like Ph-UUPh ,³ and a number of diuranium polychlorides and polyformates.⁴

In contrast to the multiple bonding between early transition metals, like, for example, the quadruple bond in $\text{K}_2[\text{Re}_2\text{Cl}_8] \cdot 2\text{H}_2\text{O}$, only rare examples of direct actinide–actinide interactions are known experimentally. There is evidence of U–U bond from gas-phase experiments⁵ or in U_2H_2 species, experimentally trapped in argon matrices.^{6,7}

The primary reaction products of laser-ablated uranium atoms with dihydrogen (UH , UH_2 , UH_3 , UH_4 , and U_2H_2) were isolated in solid argon and identified by the effects of isotopic substitution on their infrared spectra some time ago.⁷ Density functional theory (DFT) calculations were also performed to provide theoretical support for the spectral assignment.

The problem has now been revisited and several diuranium molecules with general formula U_mH_n ($m = 1, 2$; $n = 1, 2, 4, 6$) have been investigated, together with the monouranium molecules UH , UH_2 , and UH_4 . The structures of the various systems and their vibrational frequencies have been calculated to help the identification of the species present in the matrix. New experimental observations in solid hydrogen and neon will also be reported. In the attempt to identify the various species, the existence of a novel system, with formula $\text{UH}_4(\text{H}_2)_6$, was predicted. This supersystem has a potential interest as a novel metal hydride with a large number of hydrogens bound to a metal.

Theoretical and Experimental Methods

Quantum chemical calculations were performed using multiconfigurational quantum chemical methods, CASSCF/CASPT2, and DFT.

In the CASSCF/CASPT2 approach the complete active space CASSCF method⁸ is used to generate wave functions for a predetermined set of electronic states. Dynamic correlation is added using second-order perturbation theory, CASPT2.⁹

Full geometry optimization was performed for U_2H_2 , U_2H_4 , and U_2H_6 at both levels of theory, to determine the nature of the electronic ground state. At the ground state geometry, excitation energies were calculated at both levels of theory, while the vibrational frequencies, with IR intensities were calculated only at the DFT level of theory.

The CASPT2 calculations were performed using the MOL-CAS 6.4¹⁰ program package. Scalar relativistic effects were included using the Douglas–Kroll Hamiltonian and the ANO-RCC¹¹ basis set, where the primitive set 26s23p17d13f5g3h was contracted to 9s8p6d5f2g1h for uranium and the primitive set 8s4p3d was contracted to 3s2p1d for hydrogen. In the active space, molecular orbitals that are linear combinations of the 5f, 6d, and 7s orbitals of U with 1s orbitals of H were included. An active space of 10 electrons in 14 orbitals was used for U_2H_2 and U_2H_6 and an active space of 10 electrons in 12 orbitals was used for U_2H_4 . In the subsequent CASPT2 calculations, all electrons occupying up to and including the 5d orbitals of uranium were kept frozen.

The DFT calculations were performed using the ADF2005¹² program, with a basis set of QZ4P quality and the GGA-XC PBE functional.¹³ The DFT geometry optimization was followed by the calculation of harmonic frequencies, also for selected isotopic substitutes.

The matrix isolation apparatus has been described previously.¹⁴ Laser-ablated (Nd:YAG laser operating at 1064 nm, 10 Hz repetition rate, 10 ns pulse width) uranium atoms were reacted with hydrogen and isotopic samples (H_2 , D_2 , and HD) diluted in neon or pure hydrogen during co-deposition onto a 4 K substrate. In addition parahydrogen was also employed.¹⁵

* Corresponding author. E-mail: laura.gagliardi@chiphy.unige.ch.

[†] University of Geneva.

[‡] Lund University.

[§] University of Virginia.

TABLE 1: CASPT2 and DFT Structural Parameters of the Ground and the First Excited States of U_2H_2 and the Energy Difference (cm^{-1}) between the Two States

state	1A_g		3A_g	
method	CASPT2	DFT	CASPT2	DFT
$R(U-U)/\text{\AA}$	2.212	2.156	2.381	2.216
$R(U-H)/\text{\AA}$	2.003	2.059	2.024	2.105
$\angle(H-U-H)/\text{deg}$	113.0	116.9	107.9	116.5
$\Delta E(^3A_g-^1A_g)$				1406

TABLE 2: CASPT 2 and DFT Structural Parameters of the Ground and the First Excited States of U_2H_4 and the Energy Difference (cm^{-1}) between the Two States

state	$^3B_{3u}$	3B_1	1A_g	1A_g
method	CASPT2	DFT	CASPT2	DFT
$R(U-U)/\text{\AA}$	2.286	2.260	2.277	2.223
$R(U-Hb)/\text{\AA}$	2.021	2.086	2.024	2.069
$R(U-Ht)/\text{\AA}$	2.088	2.080	2.034	2.127
$\angle(H-U-H)/\text{deg}$	111.1	106.7	111.6	115.0
ΔE			1964	1905

TABLE 3: CASPT 2 and DFT Structural Parameters of the Ground and the First Excited States of U_2H_6 and the Energy Difference (cm^{-1}) between the Two States

state	1a_g	1a_g	$^3b_{1g}$	$^3B_{1g}$
method	CASPT2	DFT	CASPT2	DFT
$R(U-U)/\text{\AA}$	2.346	2.300	2.344	2.347
$R(U-Hb)/\text{\AA}$	2.042	2.089	2.083	2.128
$R(U-Ht)/\text{\AA}$	2.072	2.089	2.052	2.074
$\angle(H-U-H)/\text{deg}$	110.1	113.2	119.0	113.0
ΔE			1097	2117

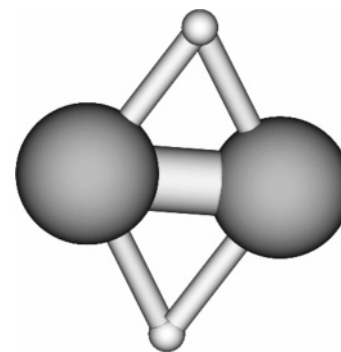
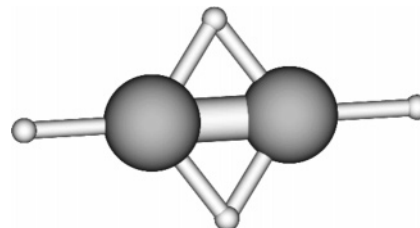
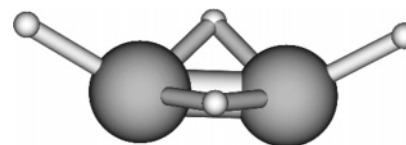
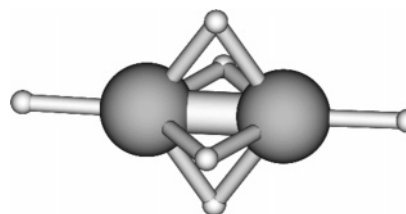
Infrared spectra were recorded on a Nicolet 550 FTIR after sample deposition, after annealing, and after irradiation using a mercury arc lamp.

Results and Discussion

The results of the calculations will be presented first, followed by new experimental observations in solid neon and hydrogen.

Structures. The structure of the ground state and the lowest excited-state of the various diuranium polyhydrides are reported in Tables 1–3. Both CASPT2 and DFT predict U_2H_2 to have a 1A_g ground state, with a rhombic D_{2h} conformation (Figure 1). D_{2h} symmetry was originally imposed during the geometry optimization. The same structure was obtained by lowering the symmetry constraints to C_{2v} in the geometry optimization. DFT predicts linear $H-UU-H$ to lie 6435 cm^{-1} higher in energy than the rhombic structure.

It is interesting to compare the electronic configurations of the formal U_2^{2+} moiety in U_2H_2 and the bare metastable cation² resulting from the CASSCF/CASPT2 calculations. The U_2^{2+} cation has a singlet ground state with a total orbital angular momentum quantum number equal to 10, corresponding to a 1N_g state. The $^1\Sigma_g^+$ state lies 279 cm^{-1} above the ground state and is very close in energy to a triplet state. The ground state of U_2^{2+} has an electronic configuration $\sigma^2\pi^4\delta_g^1\delta_u^1\varphi_u^1\varphi_g^1$ thus corresponding to a formal triple bond between the two U atoms and four fully localized electrons. In U_2H_2 the electronic configuration of the ground state, $\sigma^2\sigma^2\delta^2\pi^4$, is different from the one of U_2^{2+} , but it is similar to the one found³ for $PhUUPh$. Formally, this electronic configuration corresponds to a quintuple bond between the two uranium atoms. The effective bond order, calculated as the difference between the occupation number of the bonding orbitals, minus the occupation number of the antibonding orbitals, divided by two, is equal to 3.97, which is closer to a quadruple bond than a quintuple bond. The $U-U$ bond distance in U_2H_2 (2.21 \AA) is shorter than in U_2^{2+} (2.30 \AA)² and also than in $PhUUPh$ (2.29 \AA).³

**Figure 1.** Rhombic structure of U_2H_2 .**Figure 2.** CASPT2 optimized structure of U_2H_4 .**Figure 3.** DFT optimized structure of U_2H_4 .**Figure 4.** Structure of the ground state of U_2H_6 .

The U_2H_4 system was predicted to have a triplet ground state, $^3B_{3u}$ and 3B_1 at the CASPT2 and DFT level of theory, respectively. The CASPT2 structure is planar and has D_{2h} symmetry (Figure 2), while the DFT structure has C_{2v} symmetry, with all the hydrogens lying above the plane (Figure 3). Attempts to impose D_{2h} symmetry in the DFT calculations resulted in a structure lying 2051.1 cm^{-1} above the C_{2v} geometry, yielding imaginary values of several vibrational frequencies. Regarding other U_2H_4 isomers, DFT predicts the ethylene-like H_2U-UH_2 structure to lie 6068 cm^{-1} above the ground state and the diamond-like double-bridged structure $U-H_2-H_2-U$ to lie 13538 cm^{-1} above the ground state.

In the case of U_2H_6 , both CASPT2 and DFT level of theories predicted the double bridged (DB) 1A_g in the D_{2h} point group to be the ground state (Figure 4). This prediction was confirmed by the optimization in which only C_{2v} symmetry constraints were imposed.

Other conformations of U_2H_6 were also inspected. The ethane-like H_3U-UH_3 structure lies 5546 cm^{-1} above the DB structure. The diborane-like structure $H_2-U-H_2-U-H_2$, where the bridging and terminal hydrogen planes are perpendicular to each other, lies 18471 cm^{-1} above the DB structure (Figure 4), the planar bridged structure lies 27584 cm^{-1} above the DB structure, and the third conformation, where the terminal hydrogen planes are perpendicular to each other, lies 23784 cm^{-1} above.

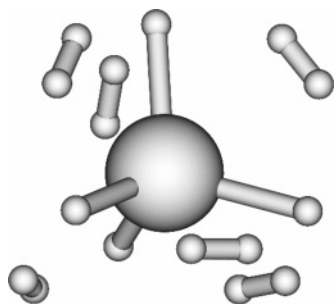


Figure 5. Structure of the ground state of $\text{UH}_4(\text{H}_2)_6$.

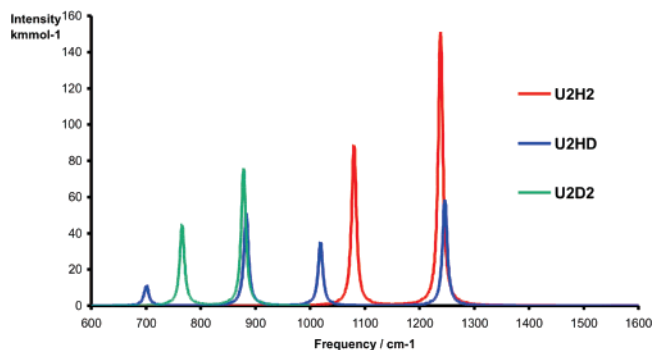


Figure 6. Calculated IR spectrum of U_2H_2 and its deuterated isotopes.

To help in the identification of the species present in the matrix, calculations were also performed on the monouranic species UH , UH_2 , and UH_4 . The typical bond distances of these species are reported in Table 4. Possible other monouranium complexes, like $\text{UH}_2(\text{H}_2)$ and $\text{UH}_4(\text{H}_2)_x$, $x = 1-6$ were also investigated and the frequencies are given in the Supporting Information (Tables 4SI–10SI). The calculations show that the species $\text{UH}_4(\text{H}_2)_6$ (Figure 5) is stable, and its experimental spectrum is discussed below. This novel species is interesting as a uranium polyhydride compound. To our knowledge sixteen is the largest number of hydrogens attached to a central metal. This compound may thus represent a new record in metal hydride chemistry. The calculated $\text{U}-\text{H}(\text{UH}_4)$ bond distance is 2.02 Å, similar to the $\text{U}-\text{H}$ bond distance of 2.01 Å for bare UH_4 (Table 4). The calculated $\text{U}-\text{H}(\text{H}_2)$ bond distance is 2.38 Å and the $\text{H}-\text{H}(\text{H}_2)$ bond distance is 0.80 Å. A similar calculation on a single H_2 molecule predicts a bond distance of 0.75 Å, indicating that the H_2 moieties interact with the U atom to form a strong complex. The structure of $\text{UH}_4(\text{H}_2)_6$ corresponds to a central UH_4 moiety surrounded by six H_2 molecules oriented along the tetrahedron edges. $\text{UH}_4(\text{H}_2)_6$ is 0.56 eV lower in energy (including zero-point-energy correction) than UH_4 and six H_2 . This energy difference indicates that the binding energy of each H_2 molecule to the central UH_4 is about 0.09 eV, an energy much stronger than ordinary solvation interaction energies (about 10 kJ/mol).

The ground state of $\text{UH}_4(\text{H}_2)_6$ is predicted to be a triplet, as in bare UH_4 .

Vibrational Frequencies. The DFT harmonic vibrational frequencies and their IR intensities for U_2H_2 , U_2H_4 , and U_2H_6 and their deuterated isotopes are reported in Tables 1SI–3SI of the Supporting Information. In the case of U_2H_6 , only the isotope in which all the six hydrogen were replaced by deuterium was considered. The plots of the calculated IR spectra for U_2H_2 , along with two possible deuterated isotopes, are reported in Figure 6, and the individual frequencies, with their intensities, of the U_2H_2 , U_2H_4 , and U_2H_6 species are available in the Supporting Information (Tables 1SI–3SI).

TABLE 4: DFT Structures of the Ground State of UH , UH_2 , and UH_4

system	UH	UH_2	UH_4
ground state	$^4\Phi$	$^3\text{B}_1$	^3A
point group	$\text{C}_{\infty\text{v}}$	$\text{C}_{2\text{v}}$	C_s
$R(\text{U}-\text{H})/\text{\AA}$	1.994	1.984	2.005
$\angle(\text{H}-\text{U}-\text{H})/\text{deg}$		114	108

TABLE 5: DFT Harmonic Vibrational Frequency (cm^{-1}) for UH , with the IR Intensity in Parentheses (km mol^{-1})

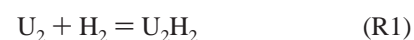
mode	UH
ν_1	1480.4 (134)
irrep	σ

TABLE 6: DFT Harmonic Vibrational Frequencies (cm^{-1}) for UH_2 and Its Deuterated Isotopes, with Their IR Intensities in Parentheses (km mol^{-1})

mode	UH_2	UHD	UD_2
ν_1	431.6 (74)	377.7 (37)	306.3 (37)
irrep	a_1	a'	a_1
ν_2	1357.7 (449)	1359.7 (389)	963.4 (226)
irrep	b_2	a'	b_2
ν_3	1361.3(272)	964.6(200)	964.6(137)
irrep	a_1	a'	a_1

Vibrational frequencies were also computed for the monouranic (UH_n , $n = 1, 2, 4, 6$) species (see Tables 5–7) and for the diuranium $\text{U}_2\text{H}_2(\text{H}_2)_2$ cluster (see Table 11SI of the Supporting Information) together with their intensities. They will help in the identification of the species present in the matrix. It is significant to note that the relative intensity of the b_{2u} and b_{1u} modes increases on interaction with the complexing H_2 submolecules. The b_{2u}/b_{1u} infrared intensity ratio in isolated U_2H_2 (1.70) increases to 2.06 in the $\text{U}_2\text{H}_2(\text{H}_2)_2$ complex, and it can be expected to go even higher with more complexing H_2 submolecules. This helps to explain the lack of experimental observation of the weaker b_{1u} mode, as will be discussed below.

Energetics. The following formation/dissociation reactions were studied at the DFT level of theory:



The calculations, including the zero-point energy corrections, show that reaction R1 is 1.7 eV exothermic, while reactions R2 and R3 are 0.3 and 0.1 eV endothermic, respectively, and reactions R4 and R5 are 5.3 and 5.8 eV endothermic, respectively. (Endothermicity and exothermicity refer to enthalpy changes.)

Experimental Observations and Discussion

The infrared spectra of the uranium and hydrogen reaction products in condensed neon are presented in Figure 7, and the observed frequencies are summarized in Table 8 and compared to previous argon matrix frequencies.⁷ Major new absorptions were observed at 1513.8, 1403.5, and 1179.4 cm^{-1} . New bands with D_2 reactions in excess neon are also given in square brackets in Table 8.

The sharp band at 1513.8 cm^{-1} shifts to 1082.4 cm^{-1} with D_2 and is assigned to the antisymmetric $\text{U}-\text{H}$ stretching fundamental of UH_4 . This band exhibits an appropriate H/D

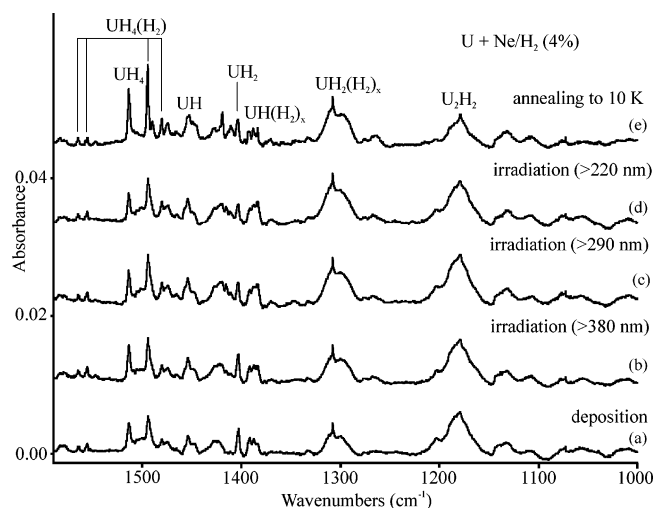
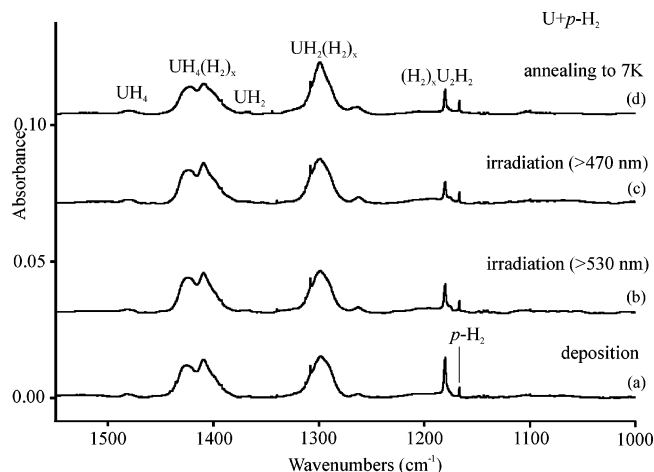
TABLE 7: DFT Harmonic Vibrational Frequencies (cm^{-1}) for UH_4 , UH_2D_2 , and UD_4 with Their IR Intensities in Parentheses (km mol^{-1})

mode	UH_4	UH_2D_2	UD_4
ν_1	224.6(331)	178.5(209)	180.4(290)
irrep	a'		a'
ν_2	366.1(249)	217.2(273)	203.3(109)
irrep	a'		a'
ν_3	366.2(263)	368.5(87)	260.7(113)
irrep	a''		a''
ν_4	590.1(9)	579.0(31)	560.3(11)
irrep	a'		a'
ν_5	601.3(1)	500.9(0)	439.5(0)
irrep	a''		a''
ν_6	1450.9(788)	1035.0(352)	1001.8(223)
irrep	a'		a'
ν_7	1454.2(670)	1051.7(244)	1033.2(343)
irrep	a''		a''
ν_8	1457.9(621)	1452.7(750)	1073.1(195)
irrep	a'		a'
ν_9	1515.9(2)	1488.7(295)	1254.4(4)
irrep	a'		a'

TABLE 8: Infrared Absorptions (cm^{-1}) for the Major Products in the Reaction of Laser-Ablated Uranium Atoms with H_2 [D_2] in Solid Argon,⁷ Hydrogen, and Neon (Present Work)

argon	hydrogen	neon	identification
		1565.0 [1117.3]	$\text{UH}_4(\text{H}_2)$
		1555.6 [1112.3]	$\text{UH}_4(\text{H}_2)$
		1547.4	UH_4 , sym
1483.6 [1060.7]	1482.8 [1056.2]	1513.8 [1082.4]	UH_4 , antisym
	1476.5 [1049.5]	1494.7 [1068.9]	$\text{UH}_4(\text{H}_2)$
1423.6 [1016.3]			UH
1403 [1000]	1426.7 [1011.8]	1453 [1038]	$\text{UH}_4(\text{H}_2)_x$
	1409.9 [1002.6]	1419 [1017]	$\text{UH}_4(\text{H}_2)_x$
1406.1 [1003.5]			UH_2 , sym str
1370.7 [978.7]	1369.5 [976.4]	1403.5 [1002.7]	UH_2 , anti sym str
1360.6 [972.5]		1392.2 [994.0]	$\text{UH}_2(\text{H}_2)$
1305 [935]	1298.7 [927.7]	1300 [935]	$\text{UH}_2(\text{H}_2)_n$
1265 [902]		1267 [900.6]	$(\text{UH}_2)_n$
1182.4 [845.6]	1180.9 [846.0]	1179.4 [844.5]	$\text{U}(\mu\text{-H}_2)\text{U}$

frequency ratio (1.412) for a very heavy metal hydride vibration and is 30 cm^{-1} higher than the argon matrix counterpart. The new HD counterparts at 1529.3 and 1000.7 cm^{-1} provide the intermediate bands for the vibrations of UH_2D_2 as described for the argon matrix spectrum.⁷ The additional band at 1494.7 cm^{-1} behaves appropriately for the analogous vibration of the $\text{UH}_4(\text{H}_2)$ complex. Indeed, DFT calculations predict that the strongest modes in this complex red shift by about 5 cm^{-1} , which is in reasonable agreement with our observations. The weaker bands at 1565.0 and 1555.6 cm^{-1} are most likely due to the UH_4 symmetric stretching mode with infrared intensity in the complex. We considered these bands for UH_6 , but this unlikely molecule is 1.8 eV higher in energy than the $\text{UH}_4(\text{H}_2)$ complex, and earlier workers have suggested that UH_6 has a low barrier to exothermic dissociation^{16,17} Experiments were done with 1, 4, and 6% H_2 in neon to look for concentration effects and more dramatic effects on annealing. We find that the 1494.7 cm^{-1} band is favored over the 1513.6 cm^{-1} band when concentration is increased and on annealing. Furthermore, we find that other bands at 1453 and 1419 cm^{-1} increased even more at higher concentration and on annealing and suggest that these are due to even higher clusters $\text{UH}_4(\text{H}_2)_x$. Finally, the sharp 1403.5 cm^{-1} band shifts to 1002.7 cm^{-1} with D_2 (H/D frequency ratio 1.400) and is 33 cm^{-1} higher than the argon matrix UH_2 band.⁷ The UHD counterparts at 1419.1 and 1014.0 cm^{-1} support this assignment. The present neon matrix absorptions for UH_4 and UH_2 provide a better prediction of the gas-phase band positions expected for these uranium hydride species.

**Figure 7.** Infrared spectra of the products of the reaction of laser-ablated U atoms with H_2 in condensing neon at 4 K: (a) after co-deposition of U and 4% H_2 in neon for 60 min; (b) after irradiation with medium-pressure mercury arc with $>380 \text{ nm}$ filter for 15 min; (c) after $>290 \text{ nm}$ irradiation; (d) after $>220 \text{ nm}$ irradiation; (e) after annealing to 10 K.**Figure 8.** Infrared spectra of the products of the reaction of laser-ablated U atoms with condensing *para*-hydrogen (99.9%) at 4 K: (a) spectrum after co-deposition of U and *p*- H_2 for 30 min; (b) after $>530 \text{ nm}$ irradiation; (c) after $>470 \text{ nm}$ irradiation; (d) after annealing to 7 K.

We must compare the observed neon matrix frequencies of UH_2 and UH_4 (1404 and 1514 cm^{-1} , respectively) as the best predictors of the gas-phase fundamentals with the present and earlier⁷ DFT frequency calculations. First, the earlier DFT calculation⁷ predicted the strong antisymmetric stretching mode of UH_2 at 1405 cm^{-1} and the present DFT calculations predict it at 1361 cm^{-1} . The difference between these two values is probably due to the different basis set used in the two calculations. Second, the calculations (old result⁷ 1472 cm^{-1} , present result 1454 cm^{-1}) for UH_4 both fall short of the observed value, which is not the usual difference found for DFT calculated harmonic and observed frequencies.¹⁸

The U reaction in *para*-hydrogen¹⁵ gave sharper product spectra than normal hydrogen, and the *para*-hydrogen spectra are shown in Figure 8. Note the sharp new absorption at 1180.6 cm^{-1} and the strong broad absorptions at 1298.6 , 1409.4 , and 1424.6 cm^{-1} . Irradiation at $>520 \text{ nm}$ reduced the sharp band by 50% and increased the broad bands by 10% and further irradiation at $>470 \text{ nm}$ decreased the sharp band another 30% with little effect on the broad bands. The band positions in normal solid hydrogen and deuterium are also listed in Table 8.

TABLE 9: DFT Frequencies (cm^{-1}) and Intensities (kmol^{-1}) of UH_4 Antisymmetric Stretching Modes in $\text{UH}_4(\text{H}_2)_n$, $n = 0-6^a$

mode	ν
UH_4	1450.9 (788)
$\text{UH}_4(\text{H}_2)$	1446.0 (572)
$\text{UH}_4(\text{H}_2)_2$	1460.0 (495)
$\text{UH}_4(\text{H}_2)_3$	1422.6 (443)
$\text{UH}_4(\text{H}_2)_4$	1422.8 (493)
$\text{UH}_4(\text{H}_2)_5$	1400.9 (372)
$\text{UH}_4(\text{H}_2)_6$	1345.0 (336)

^a The full set of frequencies is available in the Supporting Information.

The sharp absorption at 1180.6 cm^{-1} is due to U_2H_2 , based on agreement with the argon matrix band⁷ at 1182.4 cm^{-1} with its U_2D_2 counterpart at 845.6 cm^{-1} , and the present observation of U_2D_2 in solid deuterium at 846.0 cm^{-1} . Our calculations show that the isolated U_2H_2 molecule has a D_{2h} structure; however, in the presence of extra hydrogen the product observed here most likely contains coordinating H_2 molecules and opens the possibility of symmetry lowering to C_{2h} . Notice how much the 1182.4 cm^{-1} band increases on annealing in the earlier solid argon experiments.⁷ The earlier HD and $\text{H}_2 + \text{D}_2$ reactions with U in excess argon reveal two common sets of new absorptions: the first set is observed at 1220.6, 1180.4, 869.0, and 847.6 cm^{-1} , as reported previously,⁷ and the second set appears on annealing at 1201.0, 1181.5, 859.2, and 846.8 cm^{-1} . Notice that the stronger bands differ only slightly from the major pure isotopic bands at 1182.4 and 845.6 cm^{-1} . The difference between these two sets of absorptions, which is observable in the UHUD complex of lower inherent symmetry, is due to higher numbers of coordinating H_2 ligands in the $(\text{HD})_n\text{UHUD}$ - $(\text{HD})_n$ complexes. Finally, our calculation predicts two strong bands for rhombic U_2H_2 , at 1238 and 1080 cm^{-1} , and we observe only the stronger higher frequency mode (near 1182 cm^{-1}). Either the calculation overestimates the intensity of the lower mode or the matrix interaction reduces its intensity.

Another question raised by the new solid hydrogen observations is what is the product responsible for the intense broader bands at 1426.7 and 1298.7 cm^{-1} . The diuranium species U_2H_4 and U_2H_6 were considered, but these species are higher in energy than U_2H_2 plus hydrogen molecules, which makes their formation unlikely in solid hydrogen experiments. We believe that excited U atoms react with H_2 during the condensation process, but that cold U atoms dimerize to form U_2 . The diuranium molecule is then expected to activate dihydrogen spontaneously to form U_2H_2 as this reaction is calculated to be exothermic (39 kcal/mol).

Weak bands are observed in solid hydrogen at 1482.8 and 1369.5 cm^{-1} , which are near the solid argon frequencies for UH_4 and UH_2 . These bands are likely due to the UH_4 and UH_2 molecules on the surface of solid hydrogen particles. This then suggests that the strong, broad major absorptions are due to these molecules complexed by many dihydrogen molecules in the solid hydrogen matrix. Such an assignment for the strong 1298.7 cm^{-1} band is appropriate for $\text{UH}_2(\text{H}_2)_x$ even though the reaction of UH_2 and one H_2 is exothermic.⁷ However, the neon matrix band for $\text{UH}_4(\text{H}_2)$ at 1494.7 cm^{-1} is far removed from the strong 1426.7 cm^{-1} solid hydrogen band, but our calculations show that the $\text{UH}_4(\text{H}_2)_6$ super complex should red shift about 100 cm^{-1} from UH_4 itself, and the strong 1426.7 and 1409.9 cm^{-1} band in solid hydrogen is most likely due to the $\text{UH}_4(\text{H}_2)_x$ complex with x near 6. Intermediate absorptions at 1453 and 1419 cm^{-1} in solid neon are probably due to intermediate complexes with $n = 3, 4$, or 5 as our calculations (Table

9) and show that the strong UH_4 antisymmetric stretching mode decreases stepwise with the number of coordinating H_2 ligands.

Conclusions

The results of a combined quantum chemical and experimental study of several monouranium and diuranium polyhydrides have been presented. The infrared spectra of uranium and hydrogen reaction products in condensing neon has been measured and compared with previous argon matrix frequencies. The calculated molecular structures and vibrational frequencies have helped to identify the species present in the matrix. New absorptions were observed at 1513.8 and 1403.5 cm^{-1} in solid neon, and they are assigned to the monouranium-polyhydride molecules UH_2 and UH_4 . It is evident from this study that diuranium polyhydrides are also present in the matrix and some of the U_2H_2 product could arise from dimerization of UH molecules during the condensation process. The U_2H_4 and U_2H_6 molecules are not observed in solid neon and hydrogen because of the endothermic reactions with U_2H_2 and H_2 that are required for their formation. An interesting result is that, based on the infrared spectrum, UH_4 forms the large $\text{UH}_4(\text{H}_2)_6$ complex in solid hydrogen. This newly characterized compound, whose existence has been confirmed by the calculations, may represent a record in metal hydride chemistry because of the large number of hydrogen atoms binding the central uranium.

Acknowledgment. This work was supported by the Swiss National Science Foundation (grant n. 200021-111645/1) and the U.S. National Science Foundation (Grant CHE 03-52487).

Supporting Information Available: Tables of vibrational frequencies. This material is available free of charge via the Internet at <http://pubs.acs.org>.

References and Notes

- (1) (a) Gagliardi, L.; Roos, B. O. *Nature* **2005**, 433, 638. (b) Roos, B. O.; Malmqvist, P.-Å.; Gagliardi, L. *J. Am. Chem. Soc.* **2006**, 128, 17000.
- (2) Gagliardi, L.; Pyykkö, P.; Roos, B. O. *Phys. Chem. Chem. Phys.* **2005**, 7, 2415.
- (3) La Macchia, G.; Brynda, M.; Gagliardi, L. *Angew. Chem. Int.* **2006**, 45, 6210.
- (4) Roos, B. O.; Gagliardi, L. *Inorg. Chem.* **2006**, 45, 803.
- (5) Gorokhov, L. N.; Emelyanov, A. M.; Khodeev, Y. S. *Teplofizika Vysokich Temperatur* **1974**, 12, 1307.
- (6) Souter, P. F.; Kushto, G. P.; Andrews, L. *Chem. Commun.* **1996**, 21, 2401.
- (7) Souter, P. F.; Kushto, G. P.; Andrews, L.; Neurock, M. *J. Am. Chem. Soc.* **1997**, 119, 1682.
- (8) Roos, B. O. In *Advances in Chemical Physics; Ab Initio Methods in Quantum Chemistry-II*; Lawley, K. P., Ed.; John Wiley & Sons Ltd.: Chichester, England, 1987; p 399.
- (9) Andersson, K.; Malmqvist, P.-Å.; Roos, B. O. *J. Chem. Phys.* **1992**, 96, 1218.
- (10) Karlström, G.; Lindh, R.; Malmqvist, P.-Å.; Roos, B. O.; Ryde, U.; Veryazov, V.; Widmark, P.-O.; Cossi, M.; Schimmelpfennig, B.; Neogrady, P.; Seijo, L. *Comput. Mater. Sci.* **2003**, 28, 222.
- (11) Roos, B. O.; Lindh, R.; Malmqvist, P.-Å.; Veryazov, V.; Widmark, P.-O. *Chem. Phys. Lett.* **2005**, 409, 295.
- (12) (a) te Velde, G.; Bickelhaupt, F. M.; van Gisbergen, S. J. A.; Fonseca Guerra, C.; Baerends, E. J.; Snijders, J. G.; Ziegler, T. J. *Comput. Chem.* **2001**, 22, 931. (b) Fonseca Guerra, C.; Snijders, J. G.; te Velde, G.; Baerends, E. J. *Theor. Chem. Acc.* **1998**, 99, 391. (c) ADF2006.01, SCM, Theoretical Chemistry, Vrije Universiteit, Amsterdam, The Netherlands.
- (13) Perdew, J. P.; Burke, K.; Ernzerhof, M. *Phys. Rev. Lett.* **1996**, 77, 3865.
- (14) Andrews, L. *Chem. Soc. Rev.* **2004**, 33, 123 and reference therein.
- (15) Andrews, L.; Wang, X. *Rev. Sci. Instrum.* **2004**, 75, 3039.
- (16) Patzschke, M.; Pyykkö, P. *Theor. Chem. Acc.* **2003**, 109, 332.
- (17) Straka, M.; Hrobárik, P.; Kaupp, M. *J. Am. Chem. Soc.* **2005**, 127, 2591.
- (18) (a) Scott, A. P.; Radom, L. *J. Phys. Chem.* **1996**, 100, 16502. (b) Andersson, M. P.; Uvdal, P. L. *J. Phys. Chem. A* **2005**, 109, 2937.